

# On the Equivalence of Dielectric and Mechanical Dispersions in some Polymers; e.g. Poly(n-Octyl Methacrylate)\*

S. HAVRILIAK JR and S. NEGAMI†

*In a comparative study of dielectric and mechanical dispersions in polymers, the usual procedure is to compare the complex dielectric constant with the complex compliance. Using this procedure one finds that the parameters used to represent these quantities are different. However, Scaife has suggested that the polarization representation is the more fundamental way to represent dielectric relaxation processes in simple polar liquids. When his recommendations were applied to the dielectric and viscoelastic data of polymers by constructing an empirical transformation procedure for the viscoelastic process, we found that, if the viscoelastic data were so treated, a significant change in the shape of the relaxation curve occurred; although the transformed dielectric and viscoelastic data had nearly the same time parameters, the equilibrium parameters proved to be quite different. However, since in that work the dispersion data were not for the same polymer specimens, some differences in the time parameters can be expected. In this paper, we consider the dielectric data of Strella and Chinai and the viscoelastic data of Child, Dannhauser and Ferry obtained for the same sample of poly(n-octyl methacrylate). In general, the time parameters are the same and the equilibrium parameters are quite different.*

In a comparative study of dielectric and mechanical dispersions, the object is to deduce whether or not the molecular mechanisms giving rise to these two phenomena are the same. This object may be attained by comparing the molecular motional parameters of the two phenomena that are derived from experimental data and deciding whether or not they are the same. Two problems immediately arise in such a comparative study: which data yield such molecular parameters; and what molecular parameters should be compared? The customary procedure is to assume that motional parameters can be derived from the complex dielectric constant data [ $\epsilon^*(\omega)$ ]. The complex compliance [ $J^*(\omega)$ ] is chosen for comparative study rather than the complex modulus because, like  $\epsilon^*(\omega)$ , it is a retardation function. When the parameters used to represent  $\epsilon^*(\omega)$  and  $J^*(\omega)$  data are compared they are found to be quite different, e.g. the response times may differ by 3 or 4 decades in time. It is then assumed that the molecular processes must be quite different and each process is interpreted in terms of different molecular mechanisms. However, an alternate interpretation is that the comparison was not properly made.

Scaife<sup>1</sup> has criticized the use of the complex dielectric constant to represent the relaxation behaviour of simple polar liquids. He proposed that the customary method of representation be replaced by the use of the complex polarizability [ $\rho^*(\omega)$ ]. The object of this work is to extend Scaife's remarks to the comparison of dielectric and mechanical dispersions. This

\*Given in part at the IUPAC meeting, Toronto, Canada, September 1968.

†Currently a graduate student at the Chemistry Department of Kent University, Kent, Ohio.

means that the mechanical analogue of the complex polarizability which has been constructed, needs to have its parameters deduced and then compared to the complex polarizability  $\{\rho^*(\omega)\}$  parameters. In this work a comparison is made of the dielectric and mechanical dispersions in poly(*n*-octyl methacrylate). The dielectric and mechanical data on which this comparison is made were obtained from measurements on the same polymer preparation.

#### GENERAL BACKGROUND

The task of constructing the mechanical analogue of  $\rho^*(\omega)$  has been given elsewhere<sup>2</sup>. The quantity  $\delta^*(\omega)$  is referred to as the complex distortability of a unit sphere suspended in an otherwise continuous rigid medium of material constant  $J_\infty$ . This quantity is given by

$$\delta^*(\omega) = \frac{J^*(\omega) - J_\infty}{J^*(\omega) + (2/3)J_\infty} \quad (1a)$$

where  $J^*(\omega)$  is the material constant of the spherical specimen. The complex polarization is related to the complex dielectric constant  $\epsilon^*(\omega)$  by means of

$$\rho^*(\omega) = (\epsilon^*(\omega) - 1) / (\epsilon^*(\omega) + 2) \quad (1b)$$

The next aspect of this work is a consideration of how to extract motional constants from the relaxation data. It is customary to extract such constants by the method of reduced variables, a method we also used when the dispersions of poly(*n*-octyl methacrylate) were first compared. However, since that time, because of our work with other polymers<sup>3</sup> we have found two serious shortcomings in that method of representation. First of all the shape of the normalized relaxation curve is not independent of temperature, as required by the method. This observation is probably well known in the dielectric case, but it also occurs in the mechanical case. In *Figure 1* we have given a modified complex plane plot of the reduced complex compliance. The logarithmic scale was chosen because the range of  $J^*(\omega)$  is so large that we wished to prevent compressing the data into the coordinate position (0,0). The single band that is observed in the dielectric case is split into two components; one that is centred at  $15\,000 \times 10^{-10} \text{ cm}^2/\text{dyne}^*$  and the other that is centred at  $30 \times 10^{-10} \text{ cm}^2/\text{dyne}$ . As a result of this bimodal behaviour a single normalization scheme cannot be devised to take into account such behaviour. This behaviour suggests that two relaxation processes are present, an observation that is consistent with that of Ferry<sup>4</sup>. Finally a close inspection of the data reveals that the points determined at a single temperature cannot be shifted by any up-down combination to superimpose on to adjacent lines determined at neighbouring temperatures. The second criticism of this method is that shift factors, rather than relaxation times, are obtained. Shift factors are taken to be zero at the reference temperature which is arbitrarily chosen. Therefore, it is impossible to ascertain what portion of the relaxation curves are compared when one uses shift factors. As a case in point, consider the polymer

\*  $1 \text{ cm}^2/\text{dyne}$  is equivalent to  $10^{-3} \text{ m}^2/\text{N}$  (SI unit).

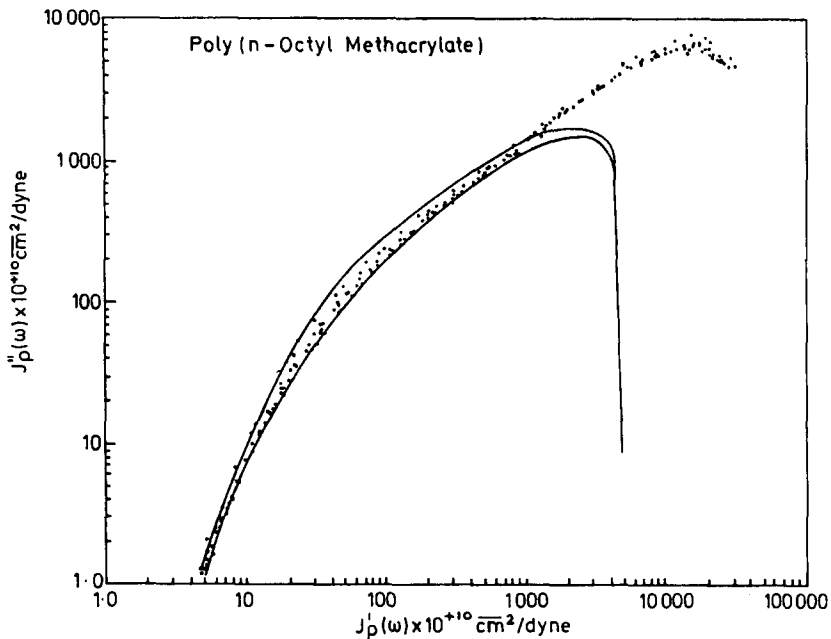


Figure 1—Complex plane plot of the normalized complex compliance. Logarithmic coordinates are used so that the experimental quantities would not be compressed into the point (0,0). (Data according to W. C. Child, W. Dannhauser and J. D. Ferry, *J. Colloid Sci.* 1958, **13**, 103)

under consideration. The mechanical and dielectric shift factors are 1.0 at the chosen reference temperature of 100°C. On the other hand, the mechanical loss becomes a maximum of 300 c/s while the dielectric loss maximum is nearly  $1.6 \times 10^7$  c/s at this temperature.

The complex plane method of data representation is chosen because these two failings are solved. In this method of data representation the real part of any complex quantity say  $R'(\omega)$  is plotted against its imaginary counterpart  $R''(\omega)$  at the same frequency. A typical complex plane plot for dielectric dispersions is linear at high frequencies and circular at low frequencies. Perhaps the most compact way of representing dielectric relaxation data is by means of the empirical relaxation function<sup>5</sup>

$$\frac{(R^*(\omega) - R_\infty)}{(R_0 - R_\infty)} = \{1 + (i\omega\tau_{0B})^{1-\alpha}\}^\beta \quad (2)$$

where the parameters  $\beta$ ,  $(1-\alpha)$ , and  $\tau_{0B}$  have been previously defined. A comparative study as suggested above reduces to a comparison of these parameters for  $\rho^*(\omega)$  data and  $\delta^*(\omega)$  data and also for  $J^*(\omega)$  data and  $\epsilon^*(\omega)$  data.

There is still one more comparison that can be made. It is a relatively simple matter to show that if the relaxation is a Debye process then the ratio of relaxation times  $\tau_\epsilon/\tau_\rho$  is given by the Lorentz field factor  $(\epsilon_0 + 2)/(\epsilon_\infty + 2)$ . The three element mechanical model which is analogous to the three element Debye model is a spring (material constant  $J_\infty$ ) in series

with a Voigt element consisting of a spring (material constant  $J_0 - J_\infty$ ) and a dash pot (material constant leading to a response time  $\tau_j$ ) in parallel. The ratio of relaxation times  $\tau_j/\tau_\delta$  is given by the mechanical analogue of the Lorentz field factor, i.e.  $3J_0/5J_\infty$ . Though these expressions cannot be solved explicitly for the empirical relaxation times in equation (2) we shall nevertheless test their validity. Specifically these relations are given by

$$\tau_{0\sigma}/\tau_{0\epsilon} = (\epsilon_\infty + 2)/(\epsilon_0 + 2) \quad (3a)$$

$$\tau_{0\sigma}/\tau_{0j} = (5/3)J_\infty/(J_0 + (2/3)J_\infty) \approx 5J_\infty/3J_0 \quad (3b)$$

#### COMPARISON OF $\epsilon^*(\omega)$ AND $J^*(\omega)$

Although the object of this work is to compare  $\rho^*(\omega)$  with  $\delta^*(\omega)$  we shall compare  $\epsilon^*(\omega)$  with  $J^*(\omega)$  in order to illustrate the limitations of this comparison. In *Figures 2a, b, c*, we have given the relaxation data<sup>6</sup> of poly(*n*-octyl methacrylate) (represented by the filled circles) obtained by Strella and Chinai at three temperatures above the glass transition temperature. The dispersion parameters are readily determined, then substituted into the dispersion equations followed by a calculation of the complex dielectric constant at the same experimental frequencies. These calculated quantities (represented by the open circles in *Figures 2a, b, c*) agree quite well with the experimental values indicating that the reliability for this method of representation is quite good. The quantities  $\psi_L$  and  $(1 - \alpha)$  were found to be temperature dependent while  $\beta$  was nearly independent of temperature (see filled circles in *Figure 3*). At a temperature of about 60°C,  $(1 - \alpha) \rightarrow 1$ , so that the relaxation process becomes the skewed semi-circle. This conclusion is in complete accord with that of Ferry<sup>5</sup>, from other arguments. The variation of the relaxation time ( $\tau_{0\epsilon}$ ) exhibits a slight curvature (see filled circles in *Figure 4*) over the entire temperature range where determinations were possible.

The set of mechanical measurements made on poly(*n*-octyl methacrylate) by Child, Dannhauser and Ferry<sup>7</sup> will be used for comparison. Despite the difficulties described in the last section, a complex plane plot of their data using a linear scale is constructed and is given in *Figure 5a*. The shape of the locus is most unlike any locus observed in dielectric dispersions. The locus appears to be a circular arc at high frequencies and is linear at low frequencies; behaviour which is opposite to the corresponding dielectric dispersion. For purposes of comparison, a curve (represented by the solid line in *Figure 5a*) was computed for a range of  $(\omega\tau_0)$ s using the mechanical values of  $J_0$  and  $J_\infty$  together with  $(1 - \alpha)$  and  $\beta$  taken from the dielectric case at these temperatures. The wide disparity between calculated and observed shapes clearly points out the differences between the two processes. The limiting angle  $\psi_L$  is 57° which is about twice the one for the dielectric process. This limiting angle is readily bisected at  $J_\infty$  and extrapolated to the locus to determine the relaxation time. Although  $\psi_L$  is expected to be temperature dependent, to a reasonable approximation this variation is not important and no attempt was made to take this change into account. The relaxation times (represented by  $\blacktriangle$  in *Figure 4* for the  $J^*(\omega)$  data) are considerably slower than the corresponding electrical one (also in *Figure 4*). It should be pointed out

EQUIVALENCE OF DIELECTRIC AND MECHANICAL DISPERSIONS

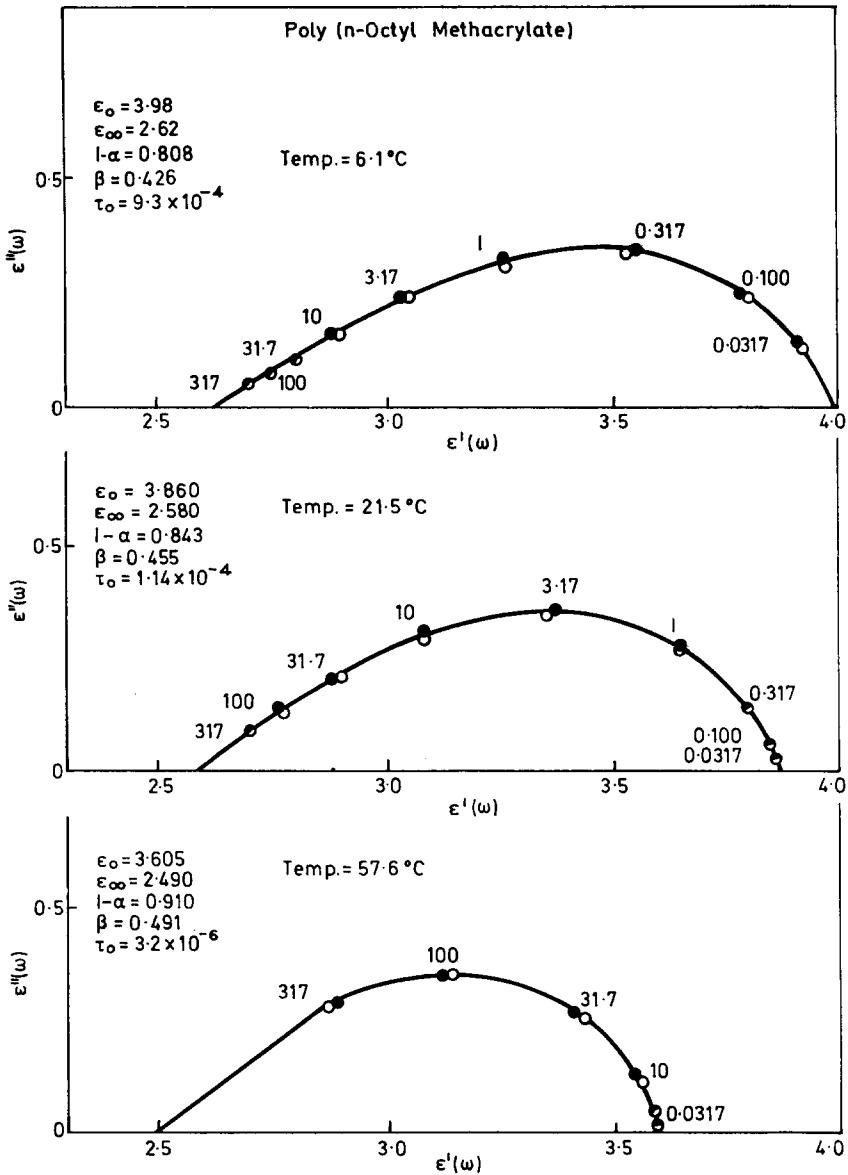


Figure 2—Complex plane plot of the complex dielectric constant for poly(n-octyl methacrylate) at three temperatures above the glass transition temperature. The filled circles are experimental quantities while the open circles were calculated at the experimental frequencies, using the parameters in the figure and equation (2).

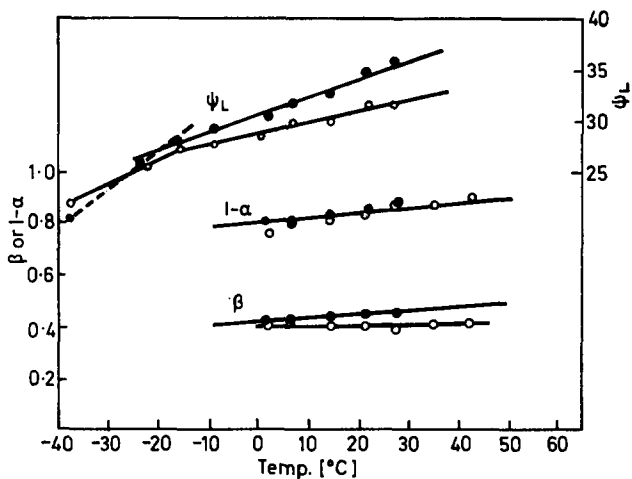


Figure 3—Variation of the three dispersion parameters [ $\psi_L$ ,  $(1-\alpha)$  and  $\beta$ ] with temperature for poly(*n*-octyl methacrylate). ●,  $\epsilon^*(\omega)$  data; ○,  $\rho^*(\omega)$  data

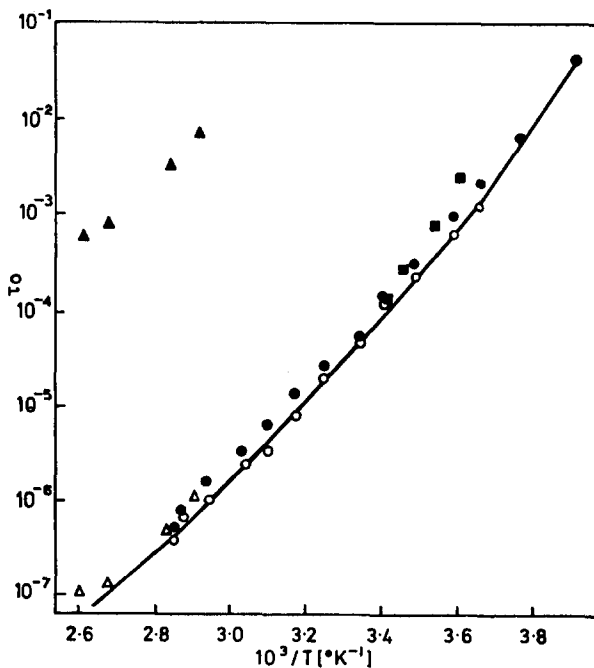


Figure 4—Variation of the relaxation time in seconds plotted against reciprocal absolute temperature for the dielectric and mechanical processes. ●,  $\epsilon^*(\omega)$  data; ○,  $\rho^*(\omega)$  data; ▲,  $J^*(\omega)$  data; △,  $(5J_\infty/3J_0)\tau_{0j}$ ; ■,  $\delta^*(\omega)$  data. (Equation of line:  $\tau_{0p} = \tau_{0e1}[(\epsilon_\infty + 2)/(\epsilon_0 + 2)]$ )

## EQUIVALENCE OF DIELECTRIC AND MECHANICAL DISPERSIONS

that the temperature dependencies are nearly the same. The equilibrium parameters as well as the instantaneous ones are also quite different in not only magnitude but in their units.

### COMPARISON OF $\rho^*(\omega)$ AND $\delta^*(\omega)$

The experimental quantities of Stella and Chinai are readily transformed into the complex polarizability by means of equation (1b). A complex plane plot of the transformed data is given in *Figures 6a, b, c*, for three temperatures above the glass transition temperatures. The dispersion parameters are readily determined and together with equation (2) are used to calculate the complex polarizability at the same frequencies as the experimental ones. The agreement between the calculated (open circles in

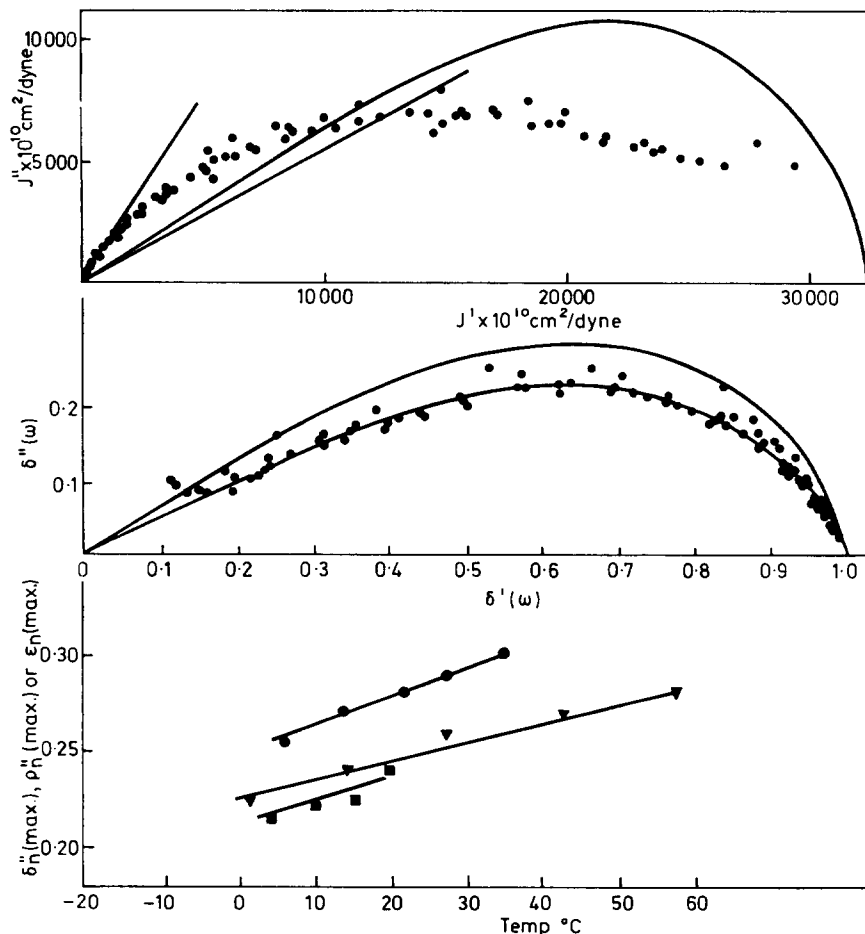


*Figure 5a*—Linear complex plane plot of the complex compliance for poly(*n*-octyl methacrylate). The line represents the shape of the corresponding dielectric process with assumed  $J_0, J_\infty$ , intercepts as described in the text

*5b*—Complex deformation for poly(*n*-octyl methacrylate)

*5c*—Normalized loss maximum for  $\epsilon^*(\omega)$  data (●),  $\delta^*(\omega)$  data (▼) and  $\rho^*(\omega)$  data (■)

Figure 6) is in excellent accord with the experimental ones indicating that the method of representation is quite good. The temperature dependence of the dispersion parameters  $\psi_L$ ,  $(1-\alpha)$  and  $\beta$  for the polarizability data is given in Figure 3 and is represented by the open circles. In general, the complex polarizability leads to a broader representation of the relaxation process than when it is represented as the complex dielectric constant. This is shown by the smaller values of  $\psi_L$ ,  $(1-\alpha)$  and  $\beta$  although the differences are not as great as those for polymers with  $J_0/J_\infty$  ratios in the range of 5 to 20. The temperature dependence of the polarizability parameters is the same as that for the complex dielectric constant in that at about  $60^\circ\text{C}$  the polarizability process becomes a skewed semi-circle. The temperature dependence of the relaxation time is represented by open circles in Figure 4. At any temperature the polarizability process is faster and can quantitatively be represented by equation (3a). The solid line in

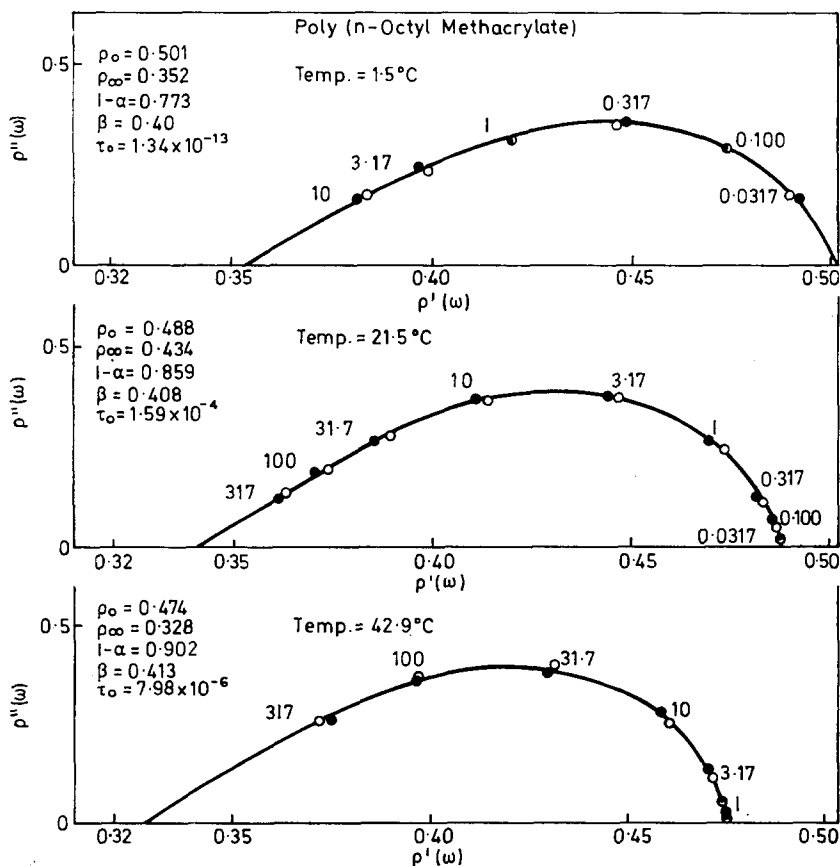


Figure 6—Complex plane plot of the complex polarization for poly(*n*-octyl methacrylate) at three temperatures above the glass transition temperature. The filled circles are experimental quantities while the open circles were calculated at the experimental frequencies using the parameters in the figure and equation (2)



*Figure 4* was calculated from the smooth relaxation time curve together with the appropriate values of  $\epsilon_0$  and  $\epsilon_\infty$ .

In order to compare  $\rho^*(\omega)$  data with  $\delta^*(\omega)$  data we proceeded as follows. The relaxation times for the  $J^*(\omega)$  data are readily converted to  $\delta^*(\omega)$  times by means of equation (3b). The results of this conversion are represented by the open triangles in *Figure 4* where it can be seen that the two times are nearly the same. The complex compliance is readily transformed to the complex distortability by means of equation (1a). The results of this computation are given in *Figure 5b* where it can be seen that the shape of the locus is nearly the same as the corresponding electrical process. The first step in the comparison is to determine the relaxation times from the data by first estimating  $\psi_L$ , then bisecting the angle, followed by an extrapolation to the experimental locus. A plot of these relaxation times is given in *Figure 4* where they are represented by the open triangles. Again we see that the relaxation times agree quite well with the electrical ones.

The next step in the comparison is of the shape parameters, i.e.  $(1-\alpha)$  and  $\beta$ . Unfortunately the frequency range of the data is not wide enough for the direct determination of those parameters so that indirect procedures must be found. One such procedure would be to calculate the curves of  $\delta^*(\omega)$  over a range of  $(\omega\tau_0)$ s by determining the intercepts with the real axis from the  $\delta^*(\omega)$  plot together with the appropriate values of  $(1-\alpha)$  and  $\beta$  taken from the corresponding dielectric case. The two lines in *Figure 5b* represent such a calculation using  $(1-\alpha)$  and  $\beta$  obtained at 14.1°C and 49.5°C which represents the highest and lowest temperatures of the  $\delta^*(\omega)$  used in this plot. We see that except for a few stray points these two lines bracket the entire spread of data points. These boundaries indicate that the locus in the  $\delta^*(\omega)$  plot is intermediate to those calculated from the dielectric data at the two temperatures.

Another comparison that can be made is to compare the normalized loss maximum for the mechanical process and compare it to the dielectric ones. Such a comparison is given in *Figure 5c* where the normalized loss maximum from the  $\epsilon^*(\omega)$ ,  $\rho^*(\omega)$  and  $\delta^*(\omega)$  data are plotted against temperature. As can be seen from *Figure 5c*, the temperature dependence of the normalized loss maximum for the  $\delta^*(\omega)$  data is the same as the corresponding dielectric ones and the absolute values of  $\delta_M''(\text{max})$  are almost (4%) the same as those from the  $\rho_M''(\text{max})$  data.

At temperatures above 50°C the  $\delta_M^*(\omega)$  data in the complex plane do not intersect the real axis at the same values ( $0.9980 \pm 0.0003$ ) rather they intersect at  $0.9995 \pm 0.0001$ . This change of intercept comes about because the locus in the complex plane is curved in such a way as to yield positive deviations from the assumed empirical behaviour. This curvature is quite marked at a temperature of 54°C while above this temperature the locus is once more quite linear. The low frequency limiting angle  $\psi_L'$  that the locus makes with the real axis is different from what is observed at lower temperatures. The parameters determined from the low temperature intercepts are given in *Table I*

Table 1. Low frequency intercepts from the complex plane

$T(^{\circ}\text{C})$	$\psi_L$	$\delta_0$
30.0	68	0.9980
34.2	70	0.9980
38.8	69	0.9980
44.0	56	0.9995
50.2	55	0.9995
54.5	54	0.9995
58.0	53	0.9993
65.8	51	0.9982

Another, perhaps more familiar way that the shape parameters can be shown to represent the high frequency portion of the relaxation process is to represent the complex compliance data in terms of the dielectric parameters  $(1-\alpha)$  and  $\beta$  together with  $J_0$  and  $J_{\infty}$  determined from the complex plane ( $\rho^*(\omega)$ ) data). This computation is conducted by first noting that the inverse of equation (1a) is given by

$$J^*(\omega) = J_{\infty} \{1 + 2\delta^*(\omega)\} / \{1 - \delta^*(\omega)\} \quad (4)$$

The quantity  $J^*(\omega)$  was computed with equation (2) for a range of  $(\omega\tau_0)$ s using  $(1-\alpha)$  and  $\beta$  taken at the required temperatures followed by inversion using equation (4).  $J^*(\omega)$  was then normalized using the data of Ferry. The results of such a calculation are given in Figure 7 for

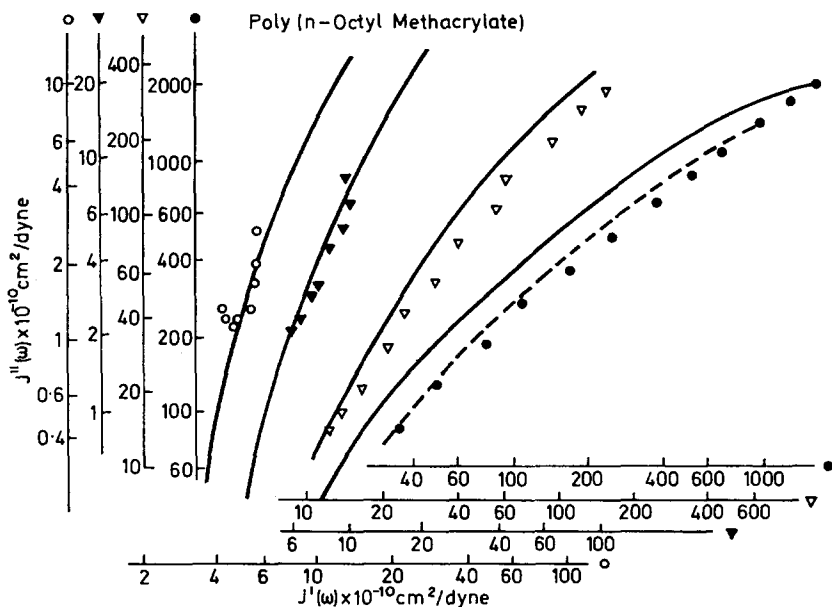


Figure 7—The complex deformation plotted in the complex plane. The symbols represent data from different temperatures as indicated in the figure. The lines represent calculated values from the dielectric parameters.  $\circ$ ,  $-9.6^{\circ}\text{C}$ ;  $\nabla$ ,  $-0.1^{\circ}\text{C}$ ;  $\bullet$ ,  $38.8^{\circ}\text{C}$

some of the temperatures in this interval and also in *Figure 1* for the two extreme temperatures. In *Figure 1* we see that the two lines bracket the entire high frequency relaxation process. We also see from this calculation that the variation of  $(1-\alpha)$  and  $\beta$  can represent the band of data occurring in this temperature range.

## DISCUSSION

The quantities  $\delta^*(\omega)$  and  $\rho^*(\omega)$ , defined by equations (1a) and (1b) are not only similar conceptually but are similarly related in form to their respective material constants. The former feature is important because it is part of the object of this work, while the latter feature is important because it maintains the conclusions of another work that was based on an empirical function. Scaife referred to the relaxation times derived from  $\rho^*(\omega)$  data as intrinsic macroscopic relaxation times. Therefore, the parameters  $(1-\alpha)$  and  $\beta$  may be referred to as a distribution of intrinsic macroscopic relaxation times. In the last section we found  $\tau_{08}$  and  $\tau_{0\rho}$  to be similar over the entire range where comparisons can be made. This is in marked contrast to  $\tau_{0\omega}$  and  $\tau_{0\epsilon}$  which differed by several decades. We also found that over a very long time scale  $(1-\alpha)$  and  $\beta$  were also similar. A similar result would have been obtained if  $\rho^*(\omega)$  parameters were replaced by  $\epsilon^*(\omega)$  parameters because the ratio  $\epsilon_0/\epsilon_\infty$  is small. In either case the agreement is such that the nature of the times ( $\tau_{08}$ ) as well as their distribution [ $(1-\alpha)$  and  $\beta$  parameters] obtained from  $\delta^*(\omega)$  data need to be discussed.

A comprehensive review of all of the evidence which relates to the extraction of molecular motional constants from dielectric constant data is beyond the scope of this paper. However, a few words concerning the underlying assumptions in the use of  $\epsilon^*(\omega)$  data does seem to be in order because of the pertinence to this work. The most comprehensive experimental study of the relationship between the macroscopic ( $\tau_{0\epsilon}$ ) and molecular ( $\tau$ ) relaxation times in polar liquids is that of Smyth<sup>8</sup>. Although not specifically stated by him, a relationship between the two times for an average polar liquid can be computed by the method of least squares and his data. This relationship is given by

$$\tau_{0\epsilon}/\tau = 1.01 + 0.0703(\epsilon_0 - \epsilon_\infty) \quad (5)$$

The line labelled L.S.F. in *Figure 8* was computed from equation (5) and we see that the ratio of the times is proportional to  $\epsilon_0 - \epsilon_\infty$ . An interesting variation of equation (5) is

$$\frac{\tau_{0\epsilon}}{\tau} = 0.35 \left( \frac{\epsilon_0 + 2}{\epsilon_\infty + 2} \right) + 0.65 \quad (6)$$

if we assume  $(\epsilon_\infty + 2) = 5$  and constant for most of the liquids studied by Smyth. In other words the ratio of relaxation times is proportional to the Lorentz field factor. The above study is for polar liquids, for our purposes such information is desirable for polar polymers; unfortunately, none is on hand so that an estimation of the numerical constant in equation (6) is not available.

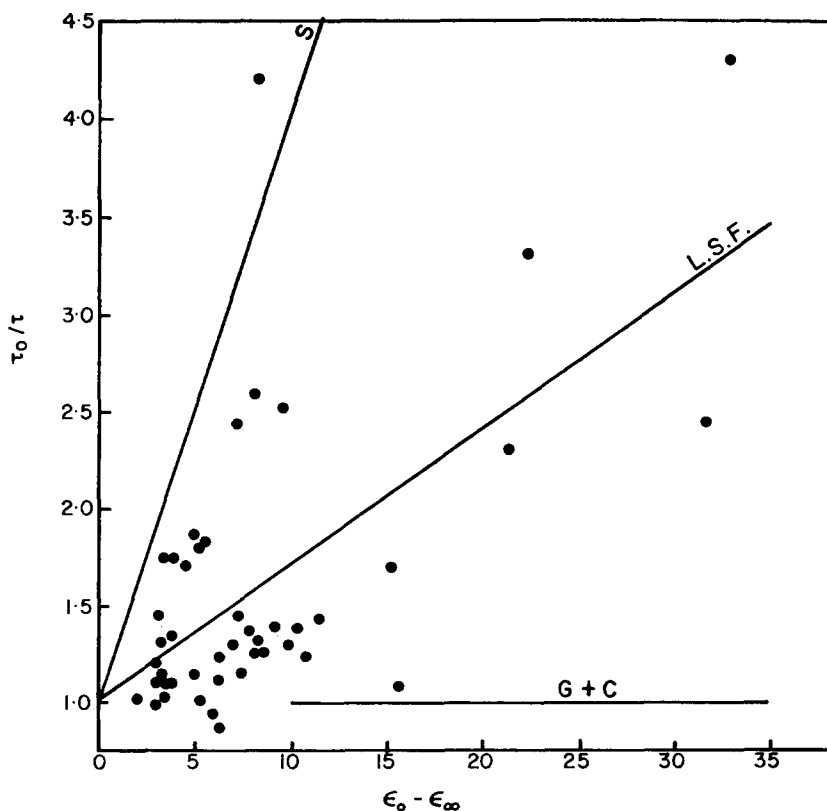


Figure 8—The Experimental ratio  $\tau_{0e}/\tau$  plotted against  $(\epsilon_0 - \epsilon_\infty)$  for a number of polar liquids. The line labelled S is obtained from Scaife; the line labelled L.S.F. is obtained by a least square fit of the data; and G+C represents the limiting value of Glarum and Cole

Both Glarum<sup>9</sup> and Cole<sup>10</sup> have developed dielectric relaxation theories based on the irreversible statistical theories of Kubo. They concluded that  $\epsilon^*(\omega)$  data yield molecular relaxation times. However, Fatuzzo and Mason<sup>11</sup> found an error in Glarum's evaluation of the macroscopic relaxation function. In as much as Cole's analysis of the macroscopic relaxation function is similar to Glarum's, it can also be criticized. Cole's analysis of the Onsager model becomes, after applying the Fatuzzo and Mason correction

$$\frac{\epsilon_0[\epsilon^*(\omega) - \epsilon_\infty][2\epsilon^*(\omega) + 1]}{\epsilon^*(\omega)[\epsilon_0 - \epsilon_\infty][2\epsilon_0 + 1]} = \mathcal{L} \left( -\frac{d\psi}{dt} \right) \quad (7)$$

where  $\mathcal{L}$  is the Laplace transform of the microscopic relaxation function  $\psi$ . Equation (7) reduces to the Fatuzzo and Mason result when  $\epsilon_\infty = 1$ . We see that the macroscopic process is no longer a simple decay when the

molecular process is an exponential decay. In the limit of large  $\epsilon_0$  and a simple microscopic decay process, equation (7) becomes

$$\epsilon^*(\omega)/\epsilon_0 = 1/(1 + i\omega\tau) \quad (8)$$

a result which is exactly the same as the one derived by Fatuzzo and Mason for the case of rigid dipoles. We see from equation (8) that not only is the macroscopic time the same as the microscopic one but they are independent of  $\epsilon_0 - \epsilon_\infty$ . The ratio  $\tau_{0e}/\tau$  for the limiting case of large  $\epsilon_0$  is given in *Figure 8* and is represented by the line labelled *G* and *C*.

Scaife concluded that  $\rho^*(\omega)$  data ought to be used for comparing relaxation data of polar liquids with widely varying equilibrium dielectric constants. Therefore if microscopic relaxation times are derived from polarizability data, then its dependence on  $\epsilon_0$  will be given by the Lorentz field factor. The line labelled *S* in *Figure 8* represents the variation of the relaxation time for such an assumption. It should be mentioned that, apart from Scaife's arguments, the derivation of molecular times for polarizability data was made by Debye using the Lorentz internal field.

The results plotted in *Figure 1* represent a most interesting state of affairs because Glarum and Cole cited Smyth's data to prove their theoretical results. We see rather, that their results form a long time limit to Smyth's estimation of molecular relaxation times  $\tau_0$  while Scaife's result forms the shorter time limit. In other words, the quantities  $\tau_{0\rho}$  and  $\tau_{0e}$  can be said to bracket nearly all of the experimental  $\tau$ s obtained by Smyth. Specifically, for nearly all of the polar liquids in *Figure 8* the following relationship can be said to be applicable.

$$\tau_{0\rho} \leq \tau \leq \tau_{0e}$$

The advantage of comparing dielectric and mechanical dispersions for polymers with small dielectric constants is now apparent. It is because the ratio  $\tau_{0e}/\tau_{0\rho}$  is small, about 1.2 for the polymer under discussion. In other words, in *Figure 4* the temperature dependence of the molecular relaxation times would be somewhere in the small band formed by the temperature dependence of  $\tau_{0\rho}$  and  $\tau_{0e}$ . We also see from *Figure 4* that over the entire temperature region that  $\tau_{0\delta}$  is within that band while  $\tau_{0J}$  is at least 3.5 decades longer. Therefore, we may conclude that molecular relaxation times may be obtained from  $\delta^*(\omega)$  data.

In a previous work<sup>3</sup> we discussed the dielectric and mechanical relaxation data of poly(*n*-hexyl methacrylate) and obtained similar results. In other words over the entire temperature range,  $\tau_{0\delta}$  times were in the band formed by  $\tau_{0\rho}$  and  $\tau_{0e}$  while  $\tau_{0J}$  was considerably slower. Therefore, we can conclude that  $\delta^*(\omega)$  data yields molecular relaxation times of this polymer while  $J^*(\omega)$  does not.

*Rohm and Haas Research Laboratories,  
Bristol,  
Pennsylvania, U.S.A.*

*(Received June 1969)*

REFERENCES

- <sup>1</sup> SCAIFE, B. K. P. *Progress in Dielectrics*, Heywood: London 1963; *Proc. phys. Soc.* 1963, **81**, 124; *Molecular Relaxation Processes*, Academic Press: London and New York, 1966
- <sup>2</sup> HAVRILIAK, S. and NEGAMI, S. *Polymer, Lond.* 1967, **8**, 161
- <sup>3</sup> HAVRILIAK, S. and NEGAMI, S. *Brit. J. Appl. Physics* 1969, **2**, 1301
- <sup>4</sup> FERRY, J. D. and STRELLA, S. *J. Colloid Sci.* 1958, **13**, 459
- <sup>5</sup> HAVRILIAK, S. and NEGAMI, S. *J. Polymer Sci. (C)* 1966, **14**, 99
- <sup>6</sup> STRELLA, S. and CHINAI, S. N. *J. Colloid Sci.* 1958, **13**, 45
- <sup>7</sup> CHILD, W. C., DANNHAUSER, W. and FERRY, J. D. *J. Colloid Sci.* 1957, **12**, 389
- <sup>8</sup> MILLER, R. C. and SMYTH, C. P. *J. Amer. Chem. Soc.* 1957, **79**, 3310
- <sup>9</sup> GLARIUM, S. H. *J. chem. Phys.* 1960, **33**, 1371
- <sup>10</sup> COLE, R. H. *J. chem. Phys.* 1965, **42**, 637
- <sup>11</sup> FATUZZO, E. and MASON, P. R. *Proc. Phys. Soc.* 1967, **90**, 741